

SUPPORT VECTOR MACHINE PROCEDURE AND GAUSSIAN MIXTURE MODELLING OF ACOUSTIC EMISSION SIGNALS TO STUDY CRACK CLASSIFICATION IN REINFORCED CONCRETE STRUCTURES

R. VIDYA SAGAR*

*Department of Civil Engineering
Indian Institute of Science, Bangalore 560 012 India
e-mail: rvsagar@iisc.ac.in

Keywords: Concrete; Crack classification; Acoustic Emission; Probability; Gaussian mixture modelling;

Abstract: Four point bending tests on reinforced concrete (RC) beam specimens were carried out and simultaneously released Acoustic Emissions (AE) were recorded in laboratory. This study reports on the AE characteristics of RC beams under monotonically increased loading. By using load-displacement curves and the AE signal parameters data, the fracture process of RC beams was studied. As the occurrence of AE events is random, a probabilistic approach named Gaussian Mixture Model (GMM) is implemented for AE data clustering related to tensile cracking and shear cracking considering different AE parameters. A supervised learning model named Support Vector Machine (SVM) procedure has been used to separate the two AE clusters belonging to tensile and shear cracks by constructing hyperplane to overcome the uncertainty. The yielding of testing specimen is compared. Influence of shear reinforcement in RC beam and type of loading was also considered in this study. The yielding of test specimen is compared for different types of loading pattern. The combination of both GMM of AE and SVM procedure to identify the exact place for separation of AE clusters are useful procedures for crack classification in concrete structures.

1 INTRODUCTION

Reinforced concrete (RC) is an indispensable material for construction of the most of civil engineering structures. In RC structures, steel bars are embedded in cement concrete so that the two materials act together to resist external forces. This combination is made to utilize the compressive strength of concrete and tensile strength of steel simultaneously. Concrete resists compression and steel reinforcement resists tensile forces. However, RC structures subjected to an external force needs monitoring for its integrity and damage condition after few years of their construction. Also, reliability and security of existing infrastructure (residential

buildings, public buildings, bridges, stadiums, tunnels, etc.) has recently received more attention. In general, periodic damage assessment of RC structures is required. Because, destruction of RC structure warns human lives and also leads to financial loss. Early assessment of material condition against large-scale failure helps to manage the structures safely and economically. One of the methods used for real time nondestructive monitoring is Acoustic Emission (AE) testing. Acoustic emission arises due to stress waves generated by mechanical deformation of material and it is the detection and analysis of these stress waves at the surface of the structure that gives rise to AE [1-4]. Intensity of crack depends on modes of cracking (tensile

and shear) in concrete structures. Different modes of cracking in concrete structures emit different AE signatures [6]. At moderate loading level tensile cracks occur and at higher loading rate shear cracks occur. Using AE parameters namely RA (=rise time/peak amplitude) and Average Frequency (AF) (=counts/duration)] values one can classify cracks (tensile and shear cracks) [6]. But occurring of cracks is random event thus researchers used probabilistic approach based on Gaussian mixture modeling to classify crack modes and further used Support Vector Machine classifier to draw hyper plane between the modes of crack [8].

2 LITERATURE REVIEW

Earlier, AE testing has been used to concrete structures for detecting the crack location [1], quantifying the status of damage [2-4] and determining the crack classification [5-7]. Quantitative evaluation of damage, crack location, shape, size, evolution can be performed in real time based on AE testing [1]. Several researchers proposed various methods that are useful to evaluate integrity and damage status of RC structures based on AE testing. Numerous studies on the damage assessment of RC structures under different loading types have been carried out. Aggelis used AE testing to study crack classification in concrete [5].

Engineers and researchers have been using stress wave testing methods namely ultrasonic pulse velocity (UPV) testing and AE testing past several years. But these test methods are used independently and separately. Limited studies have been reported on the failure mode of RC structural members by the combined usage with AE testing and ultrasonic pulse velocity methods. Farhidzadeh et al. studied classification of cracks due to bending of beam by 3 point bending test [10]. However, present research work is on classification of cracks due to uniaxial compression. Using AE parameters like RA and AF values we classified cracks (tensile and shear cracks). In fact, AE events are random in nature thus we used probabilistic approach based on Gaussian

Mixture Modelling (GMM) to classify crack modes and further used Support Vector Machine (SVM) classifier to draw hyper plane between the modes of crack [8-11].

3. Probabilistic Methods

3.1. Gaussian mixture modelling of AE

GMM is a probabilistic model that distributes a dataset into different clusters from an overall population [8]. It allows the using to distribute given data in different clusters automatically without knowing the source cluster of any particular data point. The algorithm used in GMM is called Expectation Maximization (EM). EM algorithm for GMM is based on soft closing. If the source points are unknown for a random set of data points are given from different clusters, from Gaussian distribution theorem the probability is

$$F(x) = \frac{1}{\sqrt{2\pi\sigma^2}} e^{-\frac{(x-\mu)^2}{2\sigma^2}} \quad (1)$$

In Eq. (1), μ is the mean and σ^2 is the variance, x is a random data point. Here the input data is a 2-D vector i.e.; RA versus AF.

$$X = \{x_1 = (RA_1, AF_1), \dots \dots \dots (RA_t, AF_t)\} \quad (2)$$

and the classes are {1, 2} that represent tensile and shear mode respectively. There are two clusters and the events are independent. The final equation comes as

$$\left[P\left(\frac{x}{\mu}, \Sigma\right) = \frac{1}{\sqrt{2\pi \cdot 4\Sigma}} e^{-\frac{1}{2}[(x-\mu)^T \Sigma^{-1}(x-\mu)]} \right] \quad (3)$$

Where Σ is the co-variance. Similarly, for a mixture of Gaussians also called as “Linear super-position of Gaussian’s”

$$P(x) = \sum_{k=1}^2 \pi_k N\left(\frac{x}{\mu_k}, \Sigma_k\right) \quad (4)$$

$$\pi_1 = \frac{N_1}{N} \text{ for tensile} \quad (5)$$

$$\pi_1 = \frac{N_2}{N} \text{ for shear} \quad (6)$$

And the maximum likelihood equation can be written as

$$\ln p\left(\frac{x}{\mu_k}, \Sigma_k, \pi_k\right) = \sum_{n=1}^2 \ln p(x_n) = \sum_{n=1}^N \ln \left[\sum_{k=1}^2 \pi_k N\left(\frac{x_n}{\mu_k}, \Sigma_k\right) \right] \quad (7)$$

3.2. Supervised and Unsupervised learning

Unsupervised learning is used to find groups of data points with same behavior. Any previous data is not required for this learning. One can directly classify into groups depending on, how closely the data is in variables to each other. In supervised learning the labels assigned to data are known before computation. They are being used in order to 'learn' the parameters that are really significant for those clusters. A supervised learning algorithm analyzes the training data and produces an inferred function, which can be used for mapping new examples.[10] Hence, support vector machine (a supervised method) with GMM which is unsupervised are useful to study crack classification. The schematic representation of crack classification in concrete using GMM approach is shown in Figure 1.

3.3. Support Vector Machine procedure

Support vector machine (SVM) is a supervised machine learning algorithm which is used for Classification of data. SVM has been used successfully in many problems like text (and hypertext) categorization, image classification, bioinformatics (protein classification, cancer classification) and hand-written character recognition. Here, in this study, SVM procedure is implemented to classify data acquired through AE testing while cracks propagation in a RC beam. In this algorithm, each data point is plotted in 2D space with the value of each feature being the value of each coordinate. Then classification of data points

is done by finding the hyper-plane that separates the two classes well (as shown in **Figure 2**). The goal of SVM procedure is to find the optimal hyper-plane which maximizes margin. In this section mathematics involved in SVM is presented with brief description of concept. Let the equation of hyper-plane be $W^T X=0$, where W is the normal vector to the hyper-plane and X is the data set. It is required to find the biggest margin for optimal hyper-plane. Let $w^T x+b=0$ be the equation of hyper-plane (H_0), which is assumed as optimal hyper-plane. Now let's select two other hyper-planes H_1 and H_2 with equations $w^T x+b=\delta$ and $w^T x+b=-\delta$ such that H_0 is equidistant from H_1 and H_2 . To simplify our calculations we can take $\delta=1$. Now, we should make sure that no point lies between H_1 and H_2 .

$$\text{for } x_i \text{ having class 1 } W^T X_i + b \geq 1 \quad (8)$$

$$\text{for } x_i \text{ having class -1 } W^T X_i + b \leq -1 \quad (9)$$

Combining both constraints we can write,

$$y_i = (w^T x_i + b) \geq 1 \quad (10)$$

Let k be a vector in the direction of $\frac{w}{\|w\|}$, with magnitude m , the margin value. Then

$$K = m \cdot \frac{w}{\|w\|} \quad (11)$$

Let x_0 be a point on H_2 and z_0 be a point on H_1 which implies $z_0 = x_0 + k$;

We can write, $w^T z_0 + b = 1$, $w^T x_0 + b = -1$

$$W^T (x_0 + k) + b = 1 \quad (12)$$

$$W^T \left(x_0 + \frac{W}{\|W\|} \right) + b = 1 \quad (13)$$

$$W^T \left(x_0 + \frac{\|W\|^2}{\|W\|} \right) + b = 1 \quad (14)$$

$$W^T x_0 + m \|W\| + b = 1 \quad (15)$$

$$m \frac{w}{\|w\|} = 2 \quad (16)$$

Now we know that to maximize the margin we have to minimize $\|w\|$ in other words we have to minimize $\frac{1}{2} W^T W$ subjected to the constraint $Y_i (W^T X_i + b) \geq 1$.

Such problems can be solved using Lagrange multipliers [8].

$$L(w, b, \alpha) = \frac{1}{2} W^T W - \sum_{i=1}^N \alpha_i y_i (W^T x_i + b) + \sum_{i=1}^N \alpha_i \quad (17)$$

subjected to $\alpha_i \geq 0, \quad i$ (17)

For optimum solution minimize L with respect to w and b, and maximize L with respect to α .

$$W_0 = \sum_{i=1}^N \alpha_i y_i x_i \quad (18)$$

$$\sum_{i=1}^N \alpha_i y_i = 0 \quad (19)$$

KKT conditions

$$\alpha_i = [y_i (W_0^T x_i + b_0) - 1] = 0 \quad (20)$$

Hence, it is possible to find the optimum hyper plane. Few limitations of SVM algorithm are (a) Choice of kernel function and kernel parameters and (b) High algorithmic complexity and extensive memory requirements.

4. Motivation

Generally, the damage state of RC structures is estimated on the basis of periodic diagnostic results. In fact, periodic testing of RC structures is based on visual inspection, which allows identifying the large size surface defects and deviations. To detect internal defects, the most common NDT method for periodic testing is ultrasonic pulse velocity (UPV) test. But, periodic testing is limited to measuring the strength at individual sections or locating the cracks using UPV tests and other NDT methods. However, periodic testing of a RC structure does not allow detecting of sudden changes taken place in the state between its new state and condition on inspection day. AE testing is a promising NDT method to monitor such sudden changes in real

time [1]. Very Small or microcracks cannot influence UPV, but AE testing can be used to detect and locating these small microcracks.

Previous studies [8] concluded that the GMM algorithm was capable to identify the three stages of cracking during cyclic load applied on a shear wall (i) a dominance of tensile cracks at initial stage of loading (ii) a transition stage during intermediate loading stage (iii) during occurrence of shear cracks, sudden rise in AE (iv) at the final loading stage shear cracks. The validity of such conclusions is to be studied for effects of specimen geometry, specimen ductility, loading rate, type of loading or nature of loads, sensor layout and type of material [8].

5. Aim of the study

The present study focuses on failure mode due to flexural loads applied on RC structural members subjected to (i) monotonic increasing load and (ii) incremental cyclic loads. By using the UPV method and AE testing the aim is to correlate between the AE parameters recorded during fracture process in RC beams and UPV variation which characterizes different damage state. Besides the AE testing, the change in the UPV was compared with the damage evolution. A parameter 'damage index' based on recorded UPV is proposed to quantitatively estimate the damage of RC beams at different stress levels. By combined application of these two NDT methods, in prospect, will allow the engineer to estimate the damage status and also failure mode of large RC structural elements more efficiently.

6. Experimental program

6.1. Materials and Test specimen

Ordinary portland cement (53 grade), river sand, coarse aggregate (20 mm) and water were used. The concrete mixture composition was 1:1.47:2.37 by weight per cubic metre and water/cement ratio (w/c) was 0.5. The 28-days compressive strength of the concrete was 28.2 MPa. The steel reinforcement details are given

in Table 1 and the geometrical details of the test specimens. Total five RC beams (prismatic) with rectangular cross section were tested in the laboratory. All RC beams were tested under monotonically increasing loading. Steel stirrups as shear reinforcement were provided in these three test specimens. Two RC beams (SS_SF1 and SS-SF2) which does not have shear reinforcement were also tested. These two RC beams specimens were tested in order to compare the AE characteristics during tensile failure and shear failure.

6.2. Test setup

The tests were performed using a servo controlled machine (materials test system, MTS) of 1200 kN capacity. The four-point bend tests were controlled by load control of 0.06 kN/s.

6.2.1. UPV measurement

The UPV measurements were recorded at the beginning and end of the test using Portable Ultrasonic Non-destructive Digital Indicating Test (PUNDIT) instrument. UPV was recorded before testing and after testing of the specimen. The instruments used to measure UPV consists of pulse generator and transmitter and receiver. The used transducers have frequency of 54 kHz. Because, AE waves and transmitted ultrasonic pulses should not intersect each other in a RC beam.

6.2.2. AE monitoring system

The AE signal parameters were recorded using a eight channel AE monitoring system (PAC, NJ, USA) during the failure of the RC beams. For AE signal detection, two resonant type differential AE sensors (57 kHz) with preamplifier gain of 40 dB were used. The use of two AE sensors (R6D) is usual for monitoring the AE parameters in laboratory. By using the two sensors AE hit rate and other AE parameters were recorded in laboratory conditions. Study on AE event locations (or source locations) is not attempted. A threshold of 40 dB was set to screen out surrounding

noise. The experimental setup is shown in Figure 3. The AE sensors were mounted on the test specimen in 2D planar location.

7. Results and discussion

The recorded AE signal from a burst type emission have number of basic parameters; peak amplitude, rise-time, average frequency, ring-down count and energy. Most of these are complex functions of the frequency response of the sensor and structure, damping characteristics of the sensor and propagation medium, coupling efficiency, sensor sensitivity, amplifier gain and threshold voltage. In the past, AE systems were only able to record these parameters, known as AE feature data, and not whole waveforms throughout a test, so analysis techniques were limited. The waveform parameters however, provide a good indication of the intensity or severity of any AE source and this information can be used to determine whether the structure under test is accumulating damage.

For each load interval shown in Table 3, the RA and AF were calculated from each AE signal detected. By using these parameters, AE hits are classified into tensile cracks and shear cracks by implementing GMM analysis as shown in Figure 4-Figure 5. And this classification was validated using SVM method as shown in Figure 6 – Figure 7. Tensile cracks exhibited lower RA and higher AF than shear cracks. As x-axis represents RA the tensile cluster is the left side which means its x-axis values (RA values) are less than shear cluster which is on right side. It can be observed from these plots obtained from GMM as shown in Figure 4 - Figure 5, that during initial loading stage shear contour is less observed but as it approaches failure zone, shear contours are dominant. It proves that as the specimen is entering into failure stage. In case of specimen failed in flexure, the transition state occurred in more time than in shear failure. The transition zone in case of specimen failed in shear is very small, because the specimen failed suddenly. The percentage of AE recorded at the instant of yielding is

more in case of specimen failed in shear than in case of specimen failed in flexure. In other words, more AE recorded at yielding, in case of shear type of failure than tensile type of failure. Figure 8a – Figure 8b shows the shear failure pattern in test specimen SF2 specimen. Figure 8c shows the number of hits recorded in the specimen. Figure 8d shows the UPV variation in the specimen and the damage index. It is interesting to observe that at the major crack appeared the UPV decreased and damage index increased to maximum.

8. CONCLUSIONS

1. The proposed damage index based on the recorded UPV reflect the damage of RC flexural member.
2. More AE hits were recorded at cracking locations and the same locations UPV decreased. Also at the same locations visible cracks had appeared on the surface of RC beam specimen.
3. At the initial cracking stage, AF showed an increasing trend due to the mode-I cracking in RC beams. At the instance of failure, RA exhibited sharp mode-II cracking leading to the higher RA value.
4. Shear stirrups had influenced the release of AE. At the early stage of loading, the tensile stress in steel reinforcement is less, hence the release of AE is less.

Table 1. Geometric details of the tested specimens

Specimen	Cross sectional area of steel (A_{st}) mm^2	Peak load (KN)	Deflection at Midspan (mm)		Load at first crack appeared	Test duration (minutes)	Type of failure
			At peak load	At collapse			
FF_FF1	307.9	85.13	27.03	26.95	---	36.25	Flexure
FF_FF2	307.9	84.16	31.84	40.26	---	24.27	Flexure
FF_FF3	307.9	79.63	34.26	15.33	22.69	23.34	Flexure
FF_SF1	307.9	83.77	29.1	26.68	30.89	23.36	Shear
FF_SF2	307.9	74.81	13.37	13.37	29.7	20.50	Shear

Table 2. AE parameters recorded

Specimen	AE parameters					Test duration (minutes)	Type of failure
	Hits	Absolute energy (aJ)	ring down counts (RDC)	energy (Volt-sec)	Signal strength (picovolt-sec)		
FF_FF1	174955	1.6E10	2944349	4559069	2.9E10	36.25	Flexure
FF_FF2	250101	4.0E10	2962658	5603052	3.5E10	24.27	Flexure
FF_FF3	82179	6.2E10	851407	11794778	7.3E10	23.34	Flexure
FF_SF1	177493	1.2E10	2097589	3626770	2.3E10	23.36	Shear
FF_SF2	156358	4.7E10	1850351	5333274	3.4E10	20.50	Shear

Table 3. Time intervals considered for GMM algorithm and the AE record during tensile-type cracking and shear cracking.

Specimen	Interval	Hits recorded			Hits (%)		
		Tensile cracking	Shear cracking	Mixed	Tensile cracking	Shear cracking	Mixed
FF_FF2	1(0-20 % of P_{max})	12464	833	107	92.9	6.2	0.8
	2(20-40 % of P_{max})	46104	1911	482	95.1	3.9	0.9
	3(40-60 % of P_{max})	43359	7941	3051	79.7	14.6	5.6
	4(60-80 % of P_{max})	49584	7244	2889	83.1	12.1	4.8
	5(80-100 % of P_{max})	46558	14322	4738	70.9	21.8	7.2
FF_FF3	1(0-20 % of P_{max})	1302	121	13	90.6	8.4	0.9
	2(20-40 % of P_{max})	14016	940	549	90.4	6.1	3.5
	3(40-60 % of P_{max})	7548	3746	1791	57.6	28.6	13.6
	4(60-80 % of P_{max})	7865	2829	1114	66.6	23.9	9.4
	5(80-100 % of P_{max})	21860	8974	347	70.1	28.7	1.1
FF_SF1	1(0-20 % of P_{max})	4951	339	33	93.1	6.3	0.6
	2(20-40 % of P_{max})	27948	429	105	98.1	1.5	0.3
	3(40-60 % of P_{max})	47191	4407	1848	88.3	8.2	3.4
	4(60-80 % of P_{max})	31979	5074	2209	81.4	12.9	5.6
	5(80-100 % of P_{max})	40546	4224	1970	86.7	9.1	4.2
FF_SF2	1(0-20 % of P_{max})	3482	6870	0	33.6	66.3	0
	2(20-40 % of P_{max})	27073	216	19	99.1	0.7	0.0
	3(40-60 % of P_{max})	36589	615	118	98.1	1.6	0.3
	4(60-80 % of P_{max})	31358	6647	3033	76.4	16.2	7.3
	5(80-100 % of P_{max})	36507	434	159	98.4	1.2	0.4

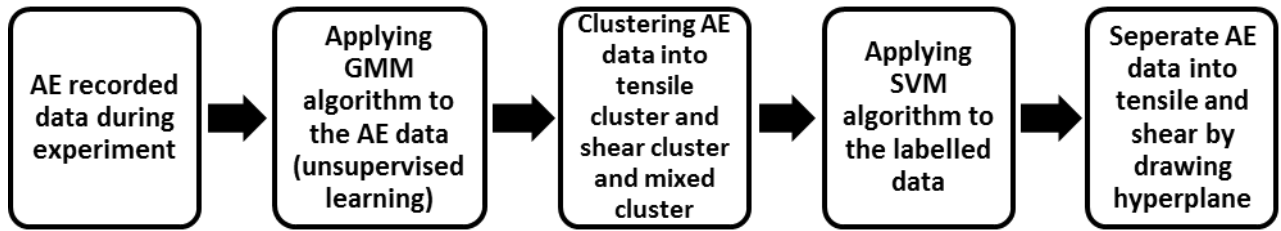


Figure 1: Schematic representation of crack classification procedure

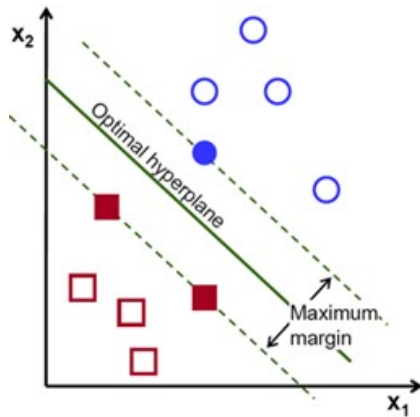


Figure 2: SVM hyper plane

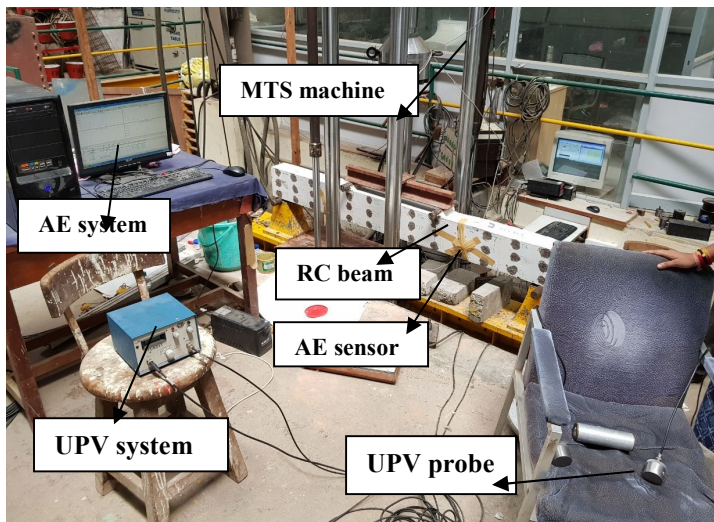
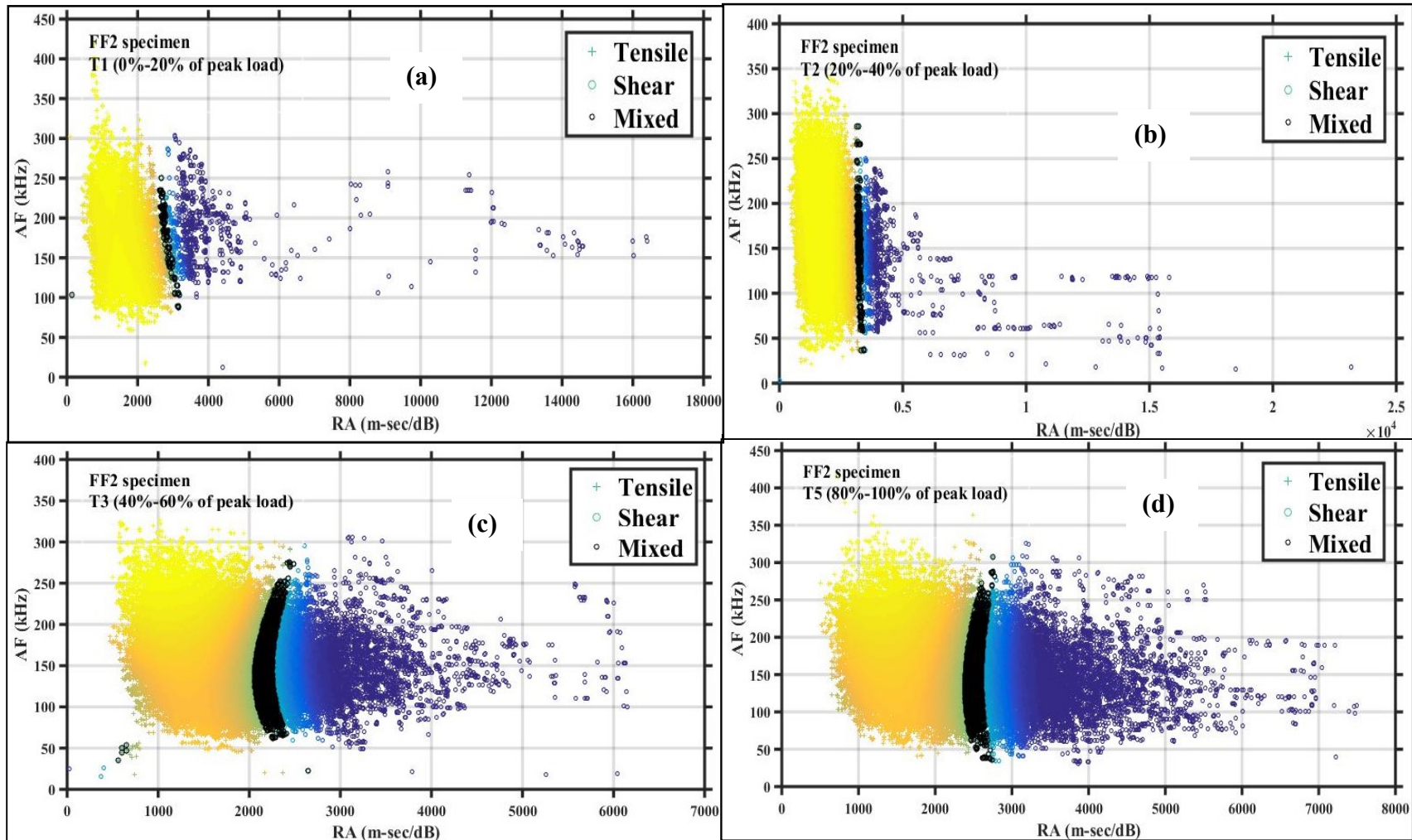


Figure 3: A RC beam specimen in the test-rig, Structures Laboratory, Department of Civil Engineering, Indian Institute of Science, Bangalore, India.

1 **Figure 4:** GMM Cluster plots for FF2 specimen (T1:0%-20% of Peak stress, T2:20%-40% of Peak stress, T3:40%-60% of Peak stress, T4:60%-
 2 80% of Peak stress, T5:80%-failure stress)
 3



4

5 **Figure 5.** GMM Cluster plots for SF2 specimen (T1:0%-20% of Peak stress, T2:20%-40% of Peak stress, T3:40%-60% of Peak stress,
6 T4:60%-80% of Peak stress, T5:80%-failure stress)

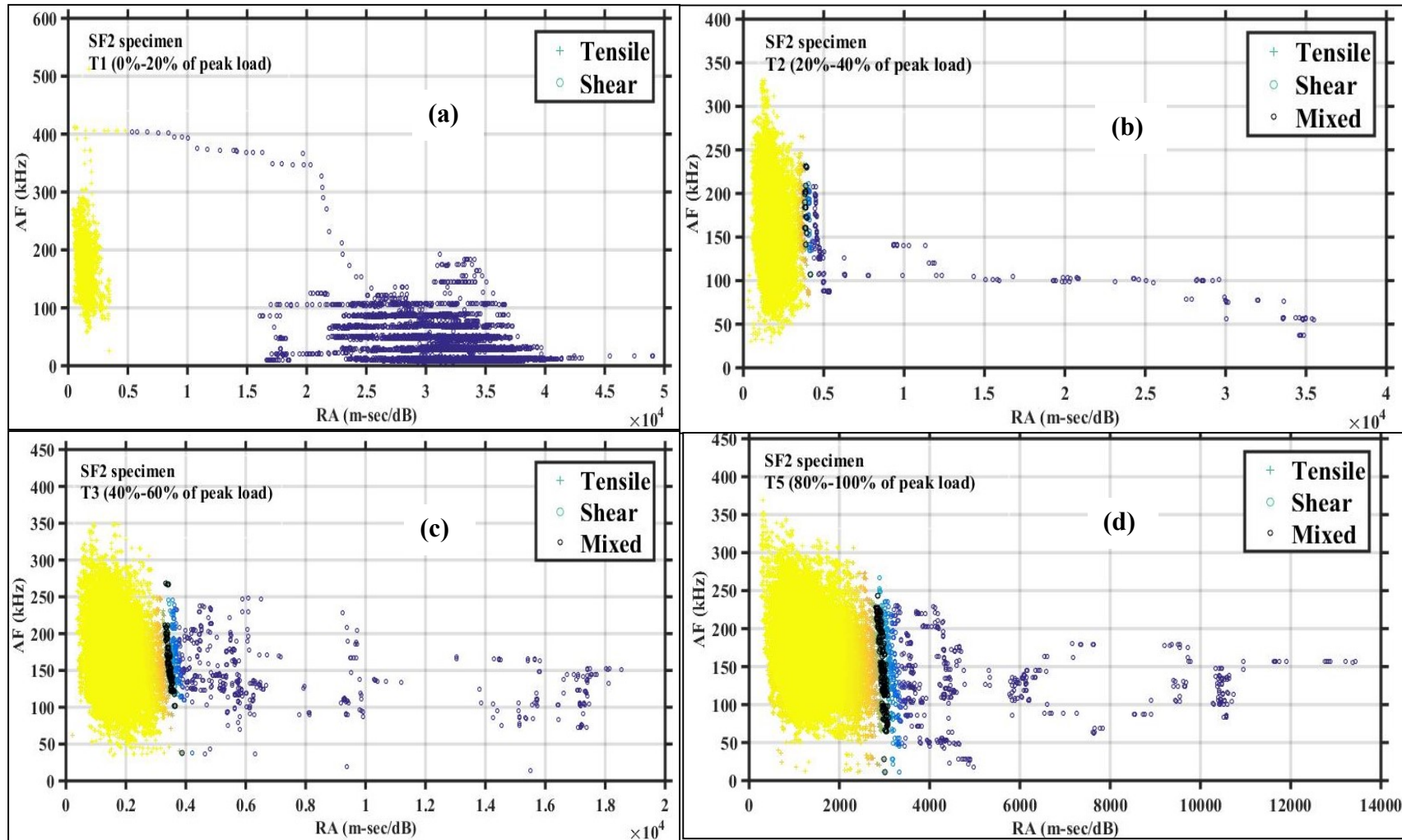


Figure 7. SVM hyperplane graphs for FF2 specimen (T1:0%-20% of Peak stress, T2:20%-40% of Peak stress, T3:40%-60% of Peak stress, T5:80%-failure from stress vs time graph).

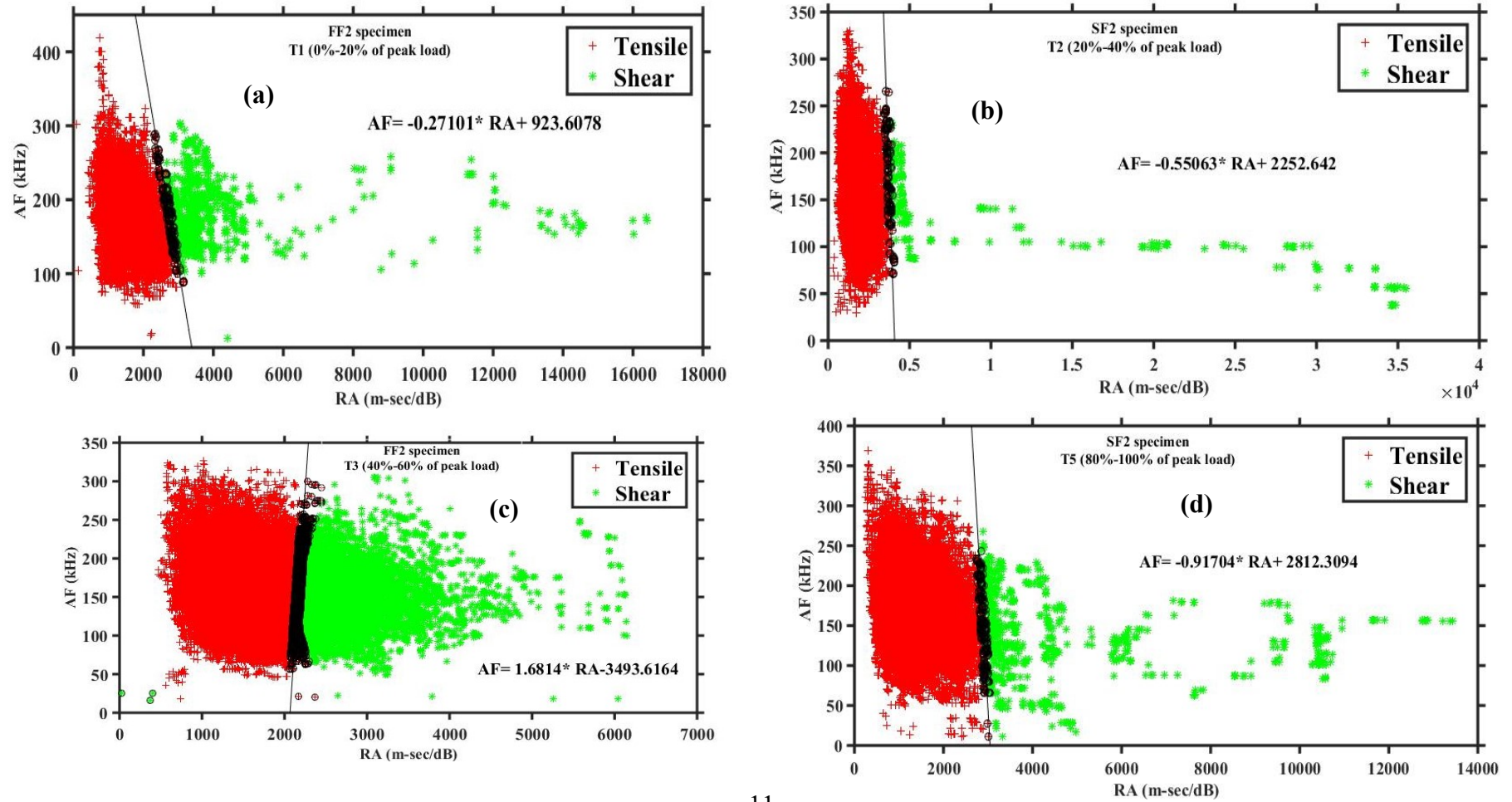
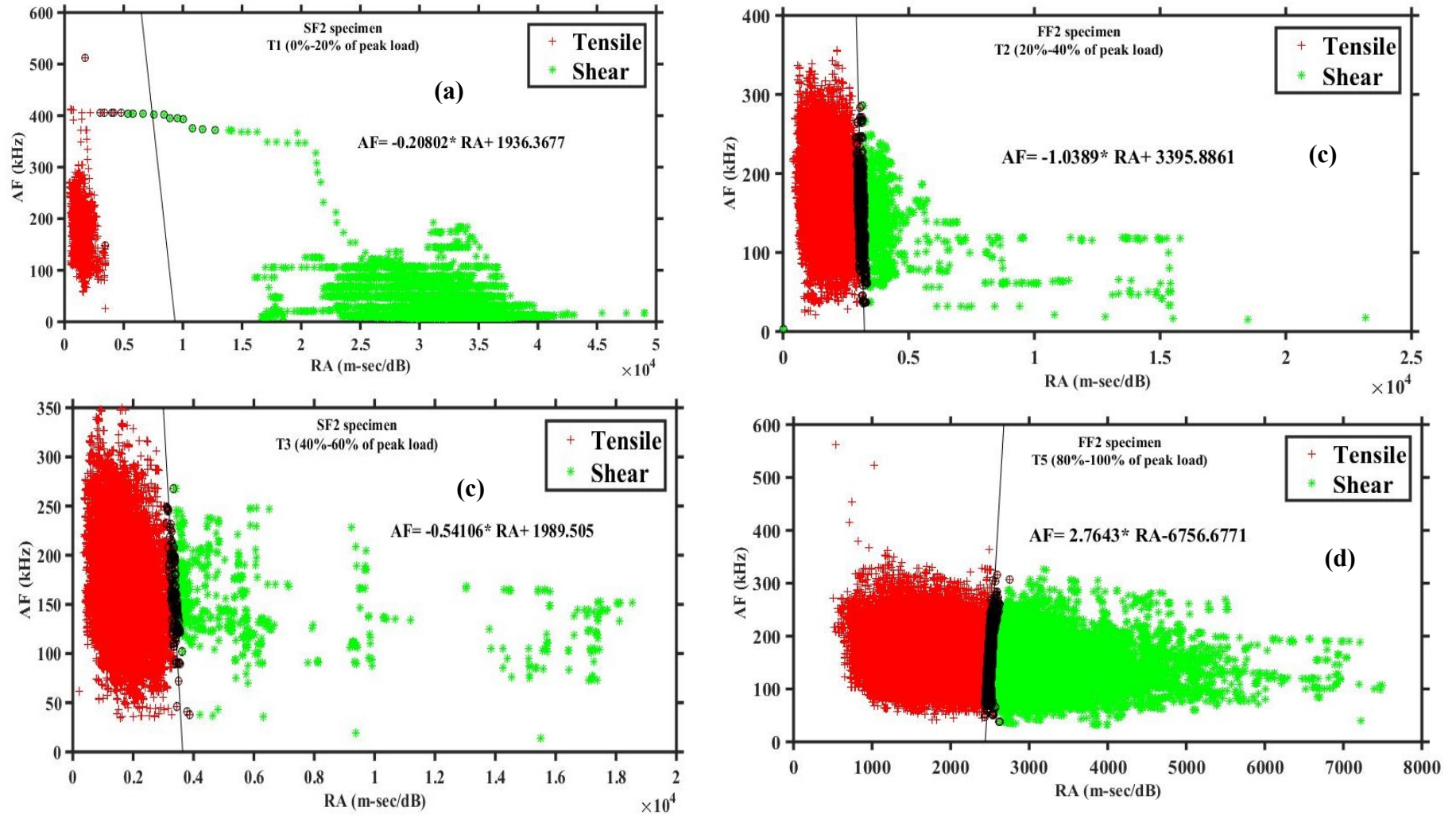


Figure 7. SVM hyperplane graphs for SF2 specimen (T1:0%-20% of Peak stress, T2:20%-40% of Peak stress, T3:40%-60% of Peak stress, T5:80%-failure from stress vs time graph)



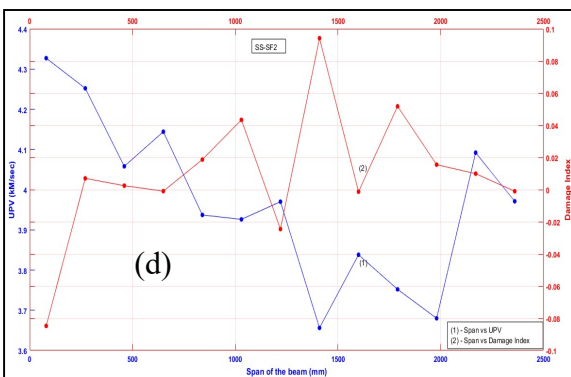
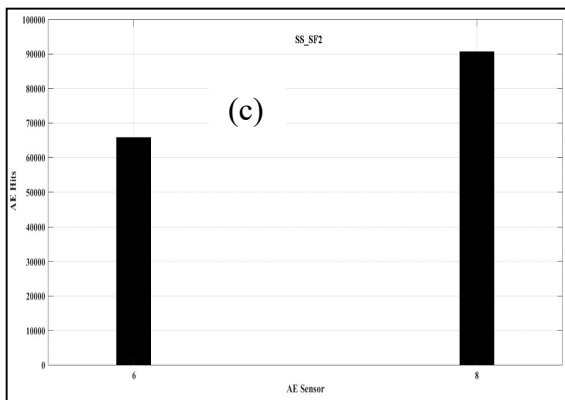


Figure 8. (a) SF2_ specimen after test. (b) formation of diagonal crack (c) AE hits recorded at each sensor (d) decrease of UPV as per crack locations.

REFERENCES

- [1] A Behnia, Chai, H.K. Shiotani, T., 2014. Advanced structural health monitoring of concrete structures with the aid of acoustic emission, *Const and Build Mat.*, **65**:282-302.
- [2]. Gross, C.U. and Ohtsu M. 2008. *Acoustic Emission Testing*. Springer-Verlag, Berlin & Heidelberg.
- [3]. Holford, K.M, Acoustic emission - Basic principles and future directions. *Strain*, **36**: 51-54.
- [4]. RILEM TC 212-ACD., 2010. Acoustic emission and related NDE techniques for crack detection and damage evaluation in concrete. Test method for classification of active cracks in concrete structures by acoustic emission. *Mat and Struct*. **43**: 1187-1189.
- [5]. Aggelis, D.G. 2011. Classification of cracking mode in concrete by acoustic emission parameters. *Mech Res Comm*. **38**:153-157.
- [6]. JCMS-III B5706., 2003. Monitoring Method for Active Cracks in Concrete by Acoustic Emission. Federation of Construction Material Industries, Japan; pp.23-28.
- [7]. Ohno, K. and Ohstu, M. 2010. Crack classification in concrete based on acoustic emission. *Const and Build Mater.*, **24**:2339-2346.
- [8]. Farhidzadeh, A. Salvatore S and Singla, P., 2013. A probabilistic approach for damage identification and crack mode classification in reinforced concrete structure. *J Int Mat Sys and Str*. **24**:1722-1735.
- [9]. Farhidzadeh A, Ehsan Dehghan-Niri, Salvatore S., 2013. Gaussian Mixture Modeling of Acoustic Emissions for Structural Health Monitoring of Reinforced Concrete Structures. *Sensors and Smart Structures Technologies for Civil, Mechanical and Aerospace Systems*.
- [10]. Farhidzadeh, A., Anastasios C, Mpalaskas, Theodore E Matikas, Farhidzadeh, H., Aggelis, D.G., 2014. Fracture mode identification in cementitious materials using supervised pattern recognition of acoustic emission features. *Const and Build Mat*. **67**:129-138.
- [11]. Reynolds D.A. and Rose R.C., 1995. Robust text-independent speaker identification using Gaussian mixture speaker models. *IEEE Transactions on Speech and Audio Processing*; **3**: 72-83.